HHS Public Access

Author manuscript

Nature. Author manuscript; available in PMC 2014 April 17.

Published in final edited form as:

Nature. 2013 October 17; 502(7471): 389–392. doi:10.1038/nature12584.

Migrating bubble during break-induced replication drives conservative DNA synthesis

Natalie Saini[2,*], **Sreejith Ramakrishnan**[1,*], **Rajula Elango**[1], **Sandeep Ayyar**[1], **Yu Zhang**[2], **Angela Deem**[1,6], **Grzegorz Ira**[4], **James E. Haber**[5], **Kirill S. Lobachev**[2,#], and **Anna Malkova**[1,3,#]

[1]Department of Biology, School of Science, IUPUI, Indianapolis, IN, 46202-5132

[2]School of Biology and Institute for Bioengineering and Bioscience, Georgia Institute of Technology, Atlanta, GA, 30332

[3]Department of Biology, College of Liberal Arts and Sciences, University of Iowa, Iowa City, IA 52242-1324

[4]Department of Molecular & Human Genetics, Baylor College of Medicine, One Baylor Plaza, Houston, Texas 77030

[5]Department of Biology and Rosenstiel Basic Medical Sciences Research Center, Waltham, Massachusetts, 02454-9110

Abstract

The repair of chromosomal double strand breaks (DSBs) is crucial in the maintenance of genomic integrity. However, the repair of DSBs can also destabilize the genome by causing mutations and chromosomal rearrangements, the driving forces for carcinogenesis and hereditary diseases. Break induced replication (BIR) is one of the DSB repair pathways that is highly prone to genetic instability[1–3]. BIR proceeds by invasion of one broken end into a homologous DNA sequence followed by replication that can copy hundreds of kilobasepairs of DNA from a donor molecule all the way through its telomere[4,5]. The resulting repaired chromosome comes at a great cost to the cell, as BIR promotes mutagenesis, loss of heterozygosity, translocations, and copy number variations, all hallmarks of carcinogenesis[4–9]. BIR employs the majority of known replication proteins to copy large portions of DNA, similar to S-phase replication[10,11]. It has thus been

[#]Correspondence and requests for materials should be addressed to AM (amalkova@iupui.edu; anna-malkova@uiowa.edu) and to KL (kirill.lobachev@biology.gatech.edu).

[6]Present address: Department of Genomic Medicine, University of Texas MD Anderson Cancer Center, Houston, TX 77230, USA.

[*]These authors contributed equally to this work.

Supplementary Information is available in the online version of the paper.

Author Contributions

SR, NS, KL and AM designed experiments. SR and AD constructed the experimental system. NS, SR, and RE carried out 2D experiments. KL, SR, AM, NS, YZ carried out molecular combing experiments. SA, RE and AD carried out experiments involving sequencing of BIR-induced mutations. RE and SA carried out experiments aimed to determine the effect of BIR on base substitutions. JEH provided key expertise. GI contributed to the studies of the role of Pif1 in BIR. NS, SR, AD, JEH, KL, and AM wrote the paper. NS and SR contributed equally to this work.

The authors declare no competing financial interests.

suggested that BIR proceeds by semiconservative replication; however, the model of a *bona-fide*, stable replication fork contradicts the known instabilities associated with BIR such as a 1000-fold increase in mutation rate compared to normal replication[9]. Here we demonstrate that the mechanism of replication during BIR is significantly different from S-phase replication, as it proceeds via an unusual bubble-like replication fork that results in conservative inheritance of the new genetic material. We provide the evidence that this atypical mode of DNA replication, dependent on Pif1 helicase, is responsible for the dramatic increase in BIR-associated mutations. We propose that the BIR-mode of synthesis presents a powerful mechanism that can initiate bursts of genetic instability in eukaryotes including humans.

Theoretically, BIR might constitute a unidirectional, *bona fide* replication fork producing two semi-conservatively replicated molecules[4,11] (Fig. 1a(i)). Alternatively, a D-loop formed by invasion of the broken chromosome may persist throughout BIR, migrating down the length of the chromosome, creating an unusual condition of conservative inheritance of newly synthesized DNA[1,12,13] (Fig. 1a(ii–iv)).

To distinguish between these models, we used a disomic yeast system (Fig. 1b(i)) containing a second, truncated copy of chromosome III (Chr III), cleaved by HO endonuclease under control of a galactose-inducible promoter[2]. The HO-induced DSB possesses only one efficiently repairable end that invades the second copy of Chr III, and initiates BIR that copies over 100 kb of the distal part of the chromosome. Using this system, we recently demonstrated that BIR stimulates mutagenesis along the path of DNA synthesis at a series of *lys2* frameshift reporters[9]. Here, we examined these Lys^+ mutations to determine whether errors during BIR were acquired semi-conservatively (inherited by either the donor or recipient molecule; Fig.1b(ii)) or conservatively (inherited only by the recipient molecule; Fig. 1b(iii)). Pulse-field gel electrophoresis (PFGE) was used to separate donor and recipient molecules from Lys^+ BIR outcomes resulting from mutations in a *lys2* reporter located 16 or 36 kb distal to the site of BIR initiation (Fig. 2a, b). Sequencing of the PCR products derived from the separated chromosomes revealed that the great majority of heterozygous frameshift mutations (58 of 58 and 68 of 77 from strains with reporters at 16 and 36 kb, respectively) were inherited by the recipient molecule, while the donor sequence remained unchanged (see also Supplementary Discussion). Overall, the mutation pattern supports a conservative replication mechanism for BIR. However, since this conclusion was based on analysis of selected mutation events, we developed a non-selective test to analyze BIR microscopically by DNA combing.

The experiments were conducted in nocodazole-arrested cells of disomic BIR strain bearing a cassette facilitating BrdU incorporation in yeast[14] (Fig. 3a, b). BrdU was added 3.5 hours following DSB induction. After completion of BIR, PFGE-separated donor and recipient molecules (Fig. 3c; Extended Data Fig. 1), were analyzed by molecular combing and fluorescent *in situ* hybridization (FISH). We used an anti-BrdU antibody, the P1 probe specific to the tandem repeat of *TEF1/BSD* inserted 14 kb centromere-proximal to *MAT* in the donor chromosome, the P2 probe specific to the 20 kb region of Chr III where invasion occurs, and the P3 probe specific to the 15 kb region near the telomere (Fig. 3a) to characterize BIR. We observed BrdU tracts approximately 100 kb in length in 70 of the 98

repaired recipient molecules analyzed (Fig. 3d, e, Extended Data Fig. 2a). These tracts include the entire chromosome region marked by P2 and P3 and, therefore, represent BIR that copied the donor chromosome through to its telomere. Additionally, 14% of recipient molecules contained long (>30 kb) BrdU tracts that overlapped with P2 but not with P3 (Fig. 3d; Extended Data Fig. 3a). These molecules likely represent repair events where BIR was interrupted, resulting in half-crossover formation[2,15] (see also Supplementary Discussion).

Our analysis of donor molecules supports a conservative mode of DNA replication during BIR, as only 4 out of 103 donor molecules were illuminated by >30 kb BrdU tracts (Fig. 3d, e; Extended Data Fig. 2a). These data confirm a strong bias ($P<0.0001$) towards BrdU tracts present only in the recipient chromosome. The 4 cases of BrdU incorporation in the donor could result from rare semi-conservative synthesis or from BIR initiated >30 kb proximal to the DSB site, which would result in a donor-like size and hybridization pattern due to copying of regions unique to the donor molecule[16]. Based on these data, we estimate that, even if semiconservative synthesis occurs, it can account for no more than 8% of the BIR events we analyzed (see Supplementary Discussion and Extended Data Fig. 4 for the results of another series of experiments supporting this conclusion).

The unusual mode of replication prompted us to characterize the structure of BIR molecular intermediates at *LYS2* inserted ~16 kb from the point of strand invasion. Genomic DNA extracted from nocodazole-arrested cells undergoing BIR was digested with PstI, and analyzed by 2-dimensional (2D) gel electrophoresis using a *LYS2*-specific probe (Fig. 4a(i)). We detected bubble-like structures between 3 and 7 hours after DSB induction (Fig. 4b–d), but not at 13 hours, consistent with the timing of BIR progression[9] (Extended Data Fig. 5). All bubble-like intermediates were markedly different from the Y structures indicative of S-phase replication forks observed before addition of nocodazole and induction of the break (Fig. 4c, 0 Hr). Furthermore, no bubble-like structures were observed in control strains in which HO endonuclease cannot initiate a DSB (Fig. 4d, No-cut), thus linking these structures to BIR exclusively. The bubble-like structures observed in BIR were reminiscent of bubbles routinely detected at replication origins[17], with one important difference: the BIR bubbles included a long, high-molecular-weight tail that extended well beyond the size expected for complete replication (arrows in Fig. 4c, d). We hypothesized that initiation of BIR lagging-strand synthesis is often delayed compared to leading strand, resulting in accumulation of single-stranded DNA (ssDNA) behind the BIR bubble, which makes the region around *LYS2* refractory to PstI digestion. Indeed, pre-incubation of genomic DNA with oligonucleotides (PstO3 and PstO4; Fig. 4a(ii, iii)) complimentary to the Watson strand of two PstI sites flanking the *LYS2* gene eliminated the tail and resulted in a second arc that likely corresponds to molecular intermediates with bubbles consisting of one double-stranded branch (leading-strand synthesis) and one single-stranded branch (lagging-strand synthesis) (Fig. 4a, b, d; Extended Data Fig. 6). Similar results were also obtained using BglII digestion (Extended Data Fig. 7). Importantly, while simultaneous addition of oligonucleotides BglO3 and BglO4, complimentary to the Watson strand of two BglII sites, eliminated the ssDNA tail, the addition of each of these oligos individually failed to eliminate the tail. This confirms that two types of DNA intermediates contribute to the observed ssDNA tail: those containing ssDNA centromere proximal to *LYS2* and those with

ssDNA distal to *LYS2* (Fig. 4a; Extended Data Fig. 7a (ii, iii)). Addition of oligonucleotides complimentary to the Crick strand did not have any effect (data not shown). Bubble migration intermediates were also detected with an *HPH*-specific probe that hybridizes to the end of the donor chromosome (Fig. 4a, e). These data strongly support a migrating D-loop type of DNA replication[18,19].

We hypothesized that ssDNA accumulated behind the migrating BIR bubble is the cause of BIR-associated mutagenesis because of the propensity of ssDNA to accumulate unrepaired DNA lesions[20]. This was tested by employing methyl methanesulfonate (MMS), a DNA damaging agent that predominantly creates mutagenic lesions in cytosines of ssDNA[21,22]. In addition, a *ura3–29* reporter[23], which can revert to Ura^+ via three different base substitutions at one C-G pair (Fig. 2c), was inserted in the donor chromosome in two different orientations (Ori1 and Ori2). We expected that MMS will specifically elevate the level of BIR-associated mutagenesis in Ori2, where cytosine is located in the mutant position of the leading (ssDNA) strand, but not in Ori1, which contains guanine instead (Fig. 2d). Indeed, we observed that even though BIR dramatically stimulated base substitutions in *ura3–29* irrespectively of its orientations, the effect of MMS was orientation-dependent (Fig. 2e; Extended Data Table 1). Specifically, MMS highly amplified BIR-induced mutagenesis in cells containing *ura3–29* in Ori2, while its effect on BIR-mutagenesis in Ori1was relatively modest. This observation supports the conjecture that ssDNA accumulated behind the BIR bubble is the cause of BIR-associated mutagenesis. Additionally, the spectrum of BIR-induced mutations was also orientation dependent, supporting our conclusion (Extended Data Fig. 2b).

Since the Pif1 helicase is a key component of the BIR machinery[24] (see also accompanying manuscript by Wilson et al.), we hypothesized that Pif1 is essential for long-range BIR. We observed that, even though BIR-sized products were formed in *pif1*Δ mutant (Extended Data Fig. 1a,b), no extended BrdU tracts were observed in either the donor or recipient chromosomes (Fig. 3d, e). In addition, approximately 22% of recipient molecules contained short (<20 kb) BrdU patches that co-localized with probe P2 (Fig. 3d, e; Extended Data Fig. 2a) and likely represented DNA synthesis that was prematurely terminated. Therefore, it is likely that the majority of outcomes in *pif1*Δ mutants formed during the time frame of these experiments were half-crossovers (Extended Data Fig. 1c), supporting our hypothesis that Pif1 is required for BIR-associated DNA synthesis. The low amount of BIR precluded 2D analysis of BIR intermediates in *pif1*Δ. We investigated whether Pif1 may be necessary for BIR-induced frameshift mutations. Strikingly, we observed that all BIR-induced frameshift mutations were eliminated in the *pif1*Δ mutant at the 36 kb position, and there was a 20-fold reduction in frameshift mutations at the 16 kb position (Fig. 2b; Extended Data Table 2). Thus, while BIR may initiate in the absence of Pif1, these data support that Pif1 is required for long-range synthesis during BIR. Therefore, Pif1 can be added to the list of other previously identified proteins, including Polδ, Polζ, Msh2, Mlh1, Dun1, and others that are involved in BIR and associated mutagenesis[2,9,10,15].

Overall, the results of this study demonstrate that BIR is carried out by a migrating bubble driven by Pif1 with asynchronous synthesis of leading and lagging strands resulting in a mutation-prone accumulation of ssDNA and leads to conservative inheritance of the new

genetic material. The bubble migration mechanism and associated mutagenesis may be relevant to cellular processes where BIR has been implicated such as alternative telomere lengthening, and mitochondria maintenance[10,25–29], where Pif1 plays an important role. An intriguing possibility is that the burst of mutations recently linked to replication stress/fork collapse in pre-cancerous cells[30] may be linked to conservative synthesis initiated by BIR.

Methods

Media, strains, and plasmids

All yeast strains (Extended Data Table 3) were isogenic to AM1003[2], which is a Chr III disome with the following genotype: *hml*Δ*::ADE1/hml*Δ*::ADE3 MAT*a-*LEU2*-tel/*MATα-inc hmr*Δ*::HPH* FS2Δ::*NAT*/FS2 *leu2/leu2-3,112 thr4 ura3–52 ade3::GAL::HO ade1 met13*.

AM1291 and AM1482 are derivatives of AM1003 and were created by deleting *LYS2* from its native location, and inserting *lys2-Ins* $A_4(A_4)$ at different positions of Chr III[9]. AM2191 and AM 2198 were constructed from AM1291 and AM1482 by replacement of *PIF1* with *KANMX* module[31]. Control strains AM1449, AM1649, AM 2247, AM2257, which contained no HO cut site in the recipient Chr III, were obtained from AM1291, AM1482, AM2191, and AM2198 as previously described[9]. AM2439 and AM2438 were created by integrating three and two copies of *TEF1/BSD-snt1* into *SNT1* of AM1291 and AM1482 respectively. The *TEF1/BSD-snt1* plasmid was constructed by cloning of a PCR-amplified 1 kb region of *SNT1* (from 185626 to 186589 positions of Chr III) into the BamHI/HindIII fragment of *TEF1/BSD* (Invitrogen). The resulting plasmid was linearized by SnaBI and integrated at *SNT1* to introduce a donor-specific region into the *MAT*α*-inc* containing copy of Chr III. The selection of transformants with integration of multiple copies of the plasmid was achieved by PFGE followed by Southern hybridization with *TEF1/BSD* used as a probe. AM2118 was isogenic to AM1247[9], but contained *KANMX* module at Chr II between *PTC4* and *TPS1*.

AM2110 is a derivative of AM1003, and was created by deleting *URA3* (using *delitto perfetto* approach) and replacing *hmr::HPH* with *hmr::KANMX*. In addition, it contains *lys2::Ins*A_4 inserted at *SED4* (36 kb centromere distal to *MATα-inc*). AM2161 and AM2820 were derivatives of AM2110 where *ura3–29-HPH* fragments (Ori1 and Ori2 respectively) were inserted 16 kb centromere distal to *MAT*α-inc between *RSC6* and *THR4*. The *ura3–29-HPH* cassettes containing *ura3–29* allele[23] in two orientations were a gift from Youri Pavlov. The insertion of *ura3–29-HPH* 16 kb centromere distal to *MATα-inc* was achieved by transformation of AM2110 with DNA fragments generated by PCR amplification of *ura3–29-HPH* using the following primers with targeting tails (uppercase) and *ura3–29-HPH* amplification sequence (lower case):
5’TCTTTCTGCAATTATTGCACGCCTCCTCGTGAGTAGTGACCGTGCGAACAAAA GAGTCATTACAACGAGGAAATAGAAGA agtcagtgagcgaggaagc3’ and
5’ATATTTGCTGCTATACTACCAAATGGAAAAATATAAGATACACAATATAGATA GTATTAAAAAAACGTGTATACGTTATT attgtactgagagtgcacc3’ Control strains AM2442, AM2259, and AM2842 which contained no HO cut site in the recipient Chr III, were obtained from AM2118, AM2161, and AM2820 as previously described[9].

AM2406 is a derivative of AM1003 that was constructed by inserting BrdU cassette (with the human equilibrative nucleoside transporter (hENT1) and the herpes simplex virus thymidine kinase)[14] into *URA3* to facilitate efficient BrdU incorporation in yeast. In particular, the p306-BrdU plasmid[14] was linearized with StuI and inserted by transformation into the *URA3* gene (Chr V). In addition, AM2406 contained insertion of three tandem arrays of the *TEF1/BSD-snt1* at *SNT1*, and replacement of *TPS1* with a *KANMX* module. *TPS1* was deleted to reduce accumulation of trehalose, which interfered with DNA purification.

Rich medium (yeast extract-peptone-dextrose [YEPD]) and synthetic complete medium, with bases and amino acids omitted as specified, were made as described[32]. YEP-raffinose, YEP-lactate and YEP-galactose were made as described[9,24]. Cultures were grown at 30°C.

Analysis of BIR efficiency

DSBs were initiated by HO induction by addition of galactose[2]. BIR efficiency was determined genetically and by physical analysis in time-course experiments using PFGE as previously described[2]. The average efficiency of BIR at each time point was calculated based on results of four independent experiments.

2D analysis of molecular intermediates of BIR

Cells were grown overnight in synthetic leucine drop-out media, transferred to YEP-raffinose, and incubated for ~16 hours, until cell density reached ~1 × 10^7 cells/ml. An aliquot was taken for analysis of the S-phase replication fork, and 2% galactose was added to induce HO endonuclease in the remainder of the culture. In these experiments, the efficiency of BIR was (80±15)%, as determined by PFGE analysis[2] 10 hours following DSB (Extended Data Fig. 5c). DSB induction led to G2/M arrest ~3 hours after galactose addition as cells were in the process of completing BIR repair (Extended Data Fig. 5d). At this point, nocodazole was added to the culture to a final concentration of 0.015 mg/ml to maintain the arrest. Cells were collected at different intervals following the break and subjected to psoralen crosslinking that allowed to constrain branch migration during DNA purification as previously described[33]. Chromosomal DNA was extracted and neutral/neutral 2D analysis was carried out according to[34]. PstI-digested DNA was separated in the first dimension on a 0.4% gel without ethidium bromide in 1X TBE buffer at 1 V/cm for 22 hours. The second dimension was run at 6 V/cm in 1X TBE buffer containing 0.3 μg/ml ethidium bromide for 12 hours.

Alternatively, to guarantee that the observed intermediates do not result from mechanical stress during genomic DNA preparation, we conducted 2D-gel electrophoresis using chromosomal DNA embedded in agarose plugs. In particular, cells collected at different intervals after induction of BIR were treated with psoralen as described in[33]. The cells were then resuspended in 750 μl solution of 1 M Sorbitol, 0.5 M EDTA (pH 8) and treated with 0.2 mg/ml lyticase for 1 hour at 37°C. The spheroplasts were washed in a solution of 50 mM Tris, 50 mM EDTA and 100 mM NaCl. The spheroplasts were then embedded in 0.8% low melt agarose at a concentration of 1.5 × 10^{10} cells/ml. The chromosomal DNA embedded in

agarose was digested with BglII, and 2D-gel electrophoresis was carried out as described for the 2D analysis of PstI-digested chromosomal DNA.

To identify regions of single-stranded DNA, a PstI or BglII digest was preceded by pre-incubation of genomic DNA with oligonucleotides that were complimentary to the PstI or BglII sites flanking the *LYS2* gene and had the following sequences: GGTCGCCCTGCAGCACAAGC (PstO3), GTCCTTTCCAGATCTTGGCAACTTT (BglO3), GCTTGTGCTGCAGGGCGACC (PstO5), AAAGTTGCCAAGATCTGGAAAGGAC (BglO5), where “O3 and “O5” indicate oligos that are complimentary to the Watson and Crick strands at the centromere-proximal site, respectively; and TAGATGGCTGCAGAACCAGT (PstO4), TGGATCTGGTAGATCTGTAAACTTGG (BglO4), ACTGGTTCTGCAGCCATCTA (PstO6), CCAAGTTTACAGATCTACCAGATCCA (BglO6), where “O4” and “O6” indicate oligos that are complimentary to the Watson and Crick strands at the telomere-proximal site, respectively.

Southern hybridization was performed using *LYS2* fragment obtained by PCR amplification of a 0.6-kb region of *LYS2* (from 471835 to 472443 kb positions of chromosome II) or using *HPH*-hybridizing fragment obtained by PCR amplification of *HPH* from the pAG32 plasmid [35].

Along with analysis of BIR intermediates, cell cycle distribution was analyzed by flow cytometry[4] and BIR kinetics were analyzed by PFGE. For PFGE, chromosome plugs were prepared[4] with genomic DNA embedded in plugs of 1% low-melting agarose and separated at 6 V/cm for 40 hours using the CHEF DRII apparatus. PFGE was followed by Southern analysis with an *ADE1*-specific probe labeled with P^{32}. Images were analyzed using a Molecular Dynamics PhosphorImager.

DNA Combing and Fluorescent In Situ Hybridization

Cells were grown overnight in synthetic leucine drop-out media , transferred to YEP-lactate, and incubated for ~20 hours, until cell density reached ~1×10^7 cells/ml. Cells were arrested by nocodazole added to 0.015 mg/ml, and DSBs were induced 2.5 hours later by addition of galactose to the final concentration of 2%. When experiments were performed according to this protocol, the efficiency of BIR was (54.0±9.8)%, as determined by PFGE analysis[2] 11 hours following DSB induction (Extended Data Fig. 1a, b). BrdU was added to the culture 3.5 hours following DSB induction by galactose to the final concentration of 0.4mg/ml after all normal DNA replication was completed but prior to the beginning of BIR. Aliquots were removed to embed cells into agarose plugs prior to and 11 hours after induction of DSBs with galactose. In experiments involving *pif1*Δ strains, the analysis was performed 13 hours following DSB induction due to slower kinetics of DSB repair in *pif1*Δ (data not shown). The uniform arrest of cells at G2/M was confirmed by the absence of BrdU incorporation in any chromosomes other than chromosome III, which was assayed by PFGE analysis of yeast chromosomes extracted from samples taken prior to the addition of BrdU and 11 or 13 h following DSB induction and probing with anti-BrdU antibodies.

Genomic DNA preparation and molecular combing were performed as described[36]. Color hybridization of Chr III molecules was performed using three fluorescent probes. P1 probe was prepared using the *TEF1/BSD* plasmid (Invitrogen) and hybridized to the 15 kb region containing three tandem repeats of the *TEF1/BSD-snt1* plasmid inserted into the donor copy of Chr III at position 186535. P2 probe marked the position close to strand invasion during BIR and was comprised of a set of four 5 kb fragments that corresponded to the following positions on the donor Chr III: 200205 to 205140, 205117 to 210385, 210361 to 215385, and 215361 to 220337. The P3 probe highlights the region close to the telomeric end of Chr III and is made up of three 5-kb fragments corresponding to the following positions on the donor chromosome: 274778 to 279801, 279778 to 284814 and 284791 to 289782. The probes were made by PCR amplification of genomic DNA from AM2406. Nucleotide sequences of the primers used to generate fragments for labeling are available upon request. Probes were labeled with biotin-dUTP. Hybridization and fluorescent detection of combed DNA molecules were achieved according to protocols described[36] with a few modifications. Successive layers of fluorophore-conjugated antibodies diluted in 1× PBST (1× PBS + 0.05% Tween) were used. For the biotin-conjugated probes, the following series was used at a dilution of 1:4000: 1) Alexa-488-Streptavidin (Molecular Probes; Life Technologies, Cat. #32354) 2) biotinylated antistreptavidin (From Vector Lab, Cat. # BA-0500), 3) Alexa-488-streptavidin, 4) biotinylated anti-streptavidin and 5) Alexa-488-Streptavidin. To detect BrdU incorporation, the following series were used at the indicated dilutions: 1) 1:20 dilution of mouse anti-BrdU (BD Biosciences, Cat. #347580), 2) 1:50 dilution of Cy3-coupled rat anti-mouse (Jackson ImmunoResearch Lab, PA; Cat. # 415-165-166) and (3) 1:50 dilution of Cy3-mouse anti-rat (Jackson ImmunoResearch Lab, PA; Cat. #212-165-168). All images were acquired using the Zeiss LSM 510 Confocal Microscope with 100× objective. The lengths of the fluorescent stretches were calculated by comparison with the length of P1, P2 and P3 hybridization signals.

The statistical comparison between donor and recipient chromosomes in respect to BrdU incorporation was performed using the Chi-square test. For each experiment, the frequency of semiconservative BIR (F) was calculated as follows: $F = A/N \times f \times b$, where A represents the number of donor molecules with long BrdU tracts; N represents the total number of analyzed donor molecules; f represents the efficiency of BIR in the experiment (calculated by physical analysis as a % of the truncated chromosome III converted in the BIR product[4]) ; and b represents the fraction of recipient molecules containing full and long interrupted BIR tracts.

Mutagenesis Associated with DSB Repair

To determine mutation frequency associated with BIR, yeast strains were grown from individual colonies with agitation in liquid synthetic media lacking leucine for approximately 20 h, diluted 20-fold with fresh YEP-Lac, and grown to logarithmic phase for approximately 16 h. Next, 20% galactose was added to the culture to a final concentration of 2%, and cells were incubated with agitation for 7 h. Samples from each culture were plated at appropriate concentrations on adenine drop-out media and on media omitting lysine and adenine before (0 h) and 7 h after the addition of galactose (7 h) to measure the frequency of Lys^+ cells. To measure the frequency of Ura^+ cells, samples were plated at appropriate

concentrations on adenine drop-out media and on media omitting uracil and adenine before (0 h) and 7 h after the addition of galactose (7 h). To determine spontaneous mutation frequencies, no-DSB strains were grown similarly to the DSB-containing strains. Because spontaneous mutation frequencies were calculated based on the number of mutations accumulated during many cell generations, the rate of spontaneous mutagenesis in no-DSB control strains was calculated using the following modification of Drake equation: $\mu=0.4343\ f/\log(N\mu)$, where μ= the rate of spontaneous mutagenesis, f= mutation frequency, and N= the number of cells in yeast culture. The rate of mutations after galactose treatment (μ_7) was determined using a simplified version of the Drake equation: $\mu_7=(f_7-f_0)$, where f_7 and f_0 are the mutation frequencies among Ade^+ cells at times 7 h and 0 h, respectively. This modification was necessary because experimental strains did not divide or underwent ≤ 1 division between 0h and 7h.

MMS was added at 1.5 mM 30 minutes after galactose addition. Cells were incubated with agitation for 7 hours, treated with 10% sodium thiosulfate to inactivate MMS, diluted and plated. The loss of viability following MMS treatment was barely detectable and never exceeded 40% independently of *ura3–29* orientation. The rate of mutations following MMS treatment was determined using simplified version of the Drake equation: $\mu_7=(f_7-f_0)$, where f_7 and f_0 are the mutation frequencies among Ade^+ cells at times 7 h (following MMS treatment) and 0 h, respectively. This modification was necessary because experimental strains did not divide or underwent ≤ 1 division between 0 h and 7 h in the presence of MMS.

Rates are reported as the median value (Fig. 2b,e; Extended Data Tables 1 and 2), and the 95% confidence limits for the median are calculated for the strains with a minimum of six individual experiments. For strains with 4–5 individual experiments, the range of the median was calculated. Statistical comparisons between median mutation rates were performed using the Mann-Whitney U test [37].

Analysis of BIR-induced Lys^+ mutants

Lys^+ revertants were obtained in BIR mutagenesis experiments[9]. After phenotypic examination, cultures were grown from mutants for chromosome analysis by PFGE using 1% low-melting agarose at 6 V/cm for 48 hours. DNA bands corresponding to the donor and repaired recipient Chr III were excised, equilibrated in β-agarase buffer (NEB), melted at 65°C, and subjected to β-agarase treatment for 1 hour at 40°C. The obtained DNA was PCR amplified using *LYS2*-specific DNA primers[9], followed by sequencing analysis.

Analysis of mutation spectra of *ura3–29* Ura^+ reversions

To determine the spectrum of Ura^+ in individual experiments, a portion of the *URA3* gene from independent Ura^+ was PCR amplified using *URA3*-specific primers: 5'GTGTGCTTCATTGGATGTTCGTAC3' and 5'AAAAGGCCTCTAGGTTCCTTTGTT3' followed by sequencing analysis using 5'CTGGAGTTAGTTGAAGCATTAGG3' as a primer.

For experimental strains undergoing BIR repair, 7h Ura^+ BIR events (confirmed as Ade^+Leu^- on selective media) were sequenced. Because these cells underwent ≤1 divisions between the 0h and 7h timepoints and the Ura^+ frequency at 7h significantly exceeded that at 0h, all Ura^+ events resulting from DSB repair were considered independent.

Supplementary Material

Refer to Web version on PubMed Central for supplementary material.

Acknowledgements

We thank Oscar Aparicio for the gift of BrdU cassette plasmid. We thank Youri Pavlov for providing *ura3–29* cassette plasmid and Paul Chastain and Anni Hangaard Andersen for providing us with reagents. We are thankful to Dmitry Gordenin and all members of AM, KL, GI, and JH laboratories for fruitful discussions throughout the work. This work was funded by grants from the US National Institutes of Health and National Science Foundation (MCB-0818122 from NSF to KL, and NIH grants R01GM084242 to AM, R01GM082950 to KL, R03ES016434 to AM and KL, GM76020 to JEH, and GM080600 to GI).

References

1. Smith CE, Llorente B, Symington LS. Template switching during break-induced replication. Nature. 2007; 447:102–105. [PubMed: 17410126]
2. Deem A, et al. Defective break-induced replication leads to half-crossovers in *Saccharomyces cerevisiae*. Genetics. 2008; 179:1845–1860. [PubMed: 18689895]
3. Malkova A, Haber JE. Mutations arising during repair of chromosome breaks. Annual review of genetics. 2012; 46:455–473.
4. Malkova A, Naylor ML, Yamaguchi M, Ira G, Haber JE. *RAD51*-dependent break-induced replication differs in kinetics and checkpoint responses from *RAD51*-mediated gene conversion. Molecular and cellular biology. 2005; 25:933–944. [PubMed: 15657422]
5. Davis AP, Symington LS. *RAD51*-dependent break-induced replication in yeast. Molecular and cellular biology. 2004; 24:2344–2351. [PubMed: 14993274]
6. Bosco G, Haber JE. Chromosome break-induced DNA replication leads to nonreciprocal translocations and telomere capture. Genetics. 1998; 150:1037–1047. [PubMed: 9799256]
7. Hastings PJ, Ira G, Lupski JR. A microhomology-mediated break-induced replication model for the origin of human copy number variation. PLoS Genet. 2009; 5:e1000327. [PubMed: 19180184]
8. Payen C, Koszul R, Dujon B, Fischer G. Segmental duplications arise from Pol32-dependent repair of broken forks through two alternative replication-based mechanisms. PLoS Genet. 2008; 4:e1000175. [PubMed: 18773114]
9. Deem A, et al. Break-induced replication is highly inaccurate. PLoS Biol. 2011; 9:e1000594. [PubMed: 21347245]
10. Lydeard JR, Jain S, Yamaguchi M, Haber JE. Break-induced replication and telomerase-independent telomere maintenance require Pol32. Nature. 2007; 448:820–823. [PubMed: 17671506]
11. Lydeard JR, et al. Break-induced replication requires all essential DNA replication factors except those specific for pre-RC assembly. Genes & development. 2010; 24:1133–1144. [PubMed: 20516198]
12. Llorente B, Smith CE, Symington LS. Break-induced replication: what is it and what is it for? Cell Cycle. 2008; 7:859–864. [PubMed: 18414031]
13. Malkova A, Ira G. Break-induced replication: functions and molecular mechanism. Current opinion in genetics & development. 2013
14. Viggiani CJ, Aparicio OM. New vectors for simplified construction of BrdU-Incorporating strains of *Saccharomyces cerevisiae*. Yeast. 2006; 23:1045–1051. [PubMed: 17083135]

15. Smith CE, Lam AF, Symington LS. Aberrant double-strand break repair resulting in half crossovers in mutants defective for Rad51 or the DNA polymerase delta complex. Molecular and cellular biology. 2009; 29:1432–1441. [PubMed: 19139272]
16. Vanhulle K, et al. Inverted DNA repeats channel repair of distant double-strand breaks into chromatid fusions and chromosomal rearrangements. Molecular and cellular biology. 2007; 27:2601–2614. [PubMed: 17242181]
17. Fangman WL, Brewer BJ. Activation of replication origins within yeast chromosomes. Annu Rev Cell Biol. 1991; 7:375–402. [PubMed: 1809350]
18. Formosa T, Alberts BM. DNA synthesis dependent on genetic recombination: characterization of a reaction catalyzed by purified bacteriophage T4 proteins. Cell. 1986; 47:793–806. [PubMed: 3022939]
19. Ferguson DO, Holloman WK. Recombinational repair of gaps in DNA is asymmetric in Ustilago maydis and can be explained by a migrating D-loop model. Proceedings of the National Academy of Sciences of the United States of America. 1996; 93:5419–5424. [PubMed: 8643590]
20. Yang Y, Sterling J, Storici F, Resnick MA, Gordenin DA. Hypermutability of damaged single-strand DNA formed at double-strand breaks and uncapped telomeres in yeast *Saccharomyces cerevisiae*. PLoS Genet. 2008; 4:e1000264. [PubMed: 19023402]
21. Yang Y, Gordenin DA, Resnick MA. A single-strand specific lesion drives MMS-induced hyper-mutability at a double-strand break in yeast. DNA repair. 2010; 9:914–921. [PubMed: 20663718]
22. Roberts SA, et al. Clustered mutations in yeast and in human cancers can arise from damaged long single-strand DNA regions. Molecular cell. 2012; 46:424–435. [PubMed: 22607975]
23. Shcherbakova PV, Pavlov YI. 3'-->5' exonucleases of DNA polymerases epsilon and delta correct base analog induced DNA replication errors on opposite DNA strands in *Saccharomyces cerevisiae*. Genetics. 1996; 142:717–726. [PubMed: 8849882]
24. Chung WH, Zhu Z, Papusha A, Malkova A, Ira G. Defective resection at DNA double-strand breaks leads to de novo telomere formation and enhances gene targeting. PLoS Genet. 2010; 6:e1000948. [PubMed: 20485519]
25. Hashimoto Y, Costanzo V. Studying DNA replication fork stability in *Xenopus* egg extract. Methods Mol Biol. 2011; 745:437–445. [PubMed: 21660709]
26. Pohjoismaki JL, Goffart S. Of circles, forks and humanity: Topological organisation and replication of mammalian mitochondrial DNA. BioEssays : news and reviews in molecular, cellular and developmental biology. 2011; 33:290–299.
27. Le S, Moore JK, Haber JE, Greider CW. *RAD50* and *RAD51* define two pathways that collaborate to maintain telomeres in the absence of telomerase. Genetics. 1999; 152:143–152. [PubMed: 10224249]
28. Kreuzer KN, Saunders M, Weislo LJ, Kreuzer HW. Recombination-dependent DNA replication stimulated by double-strand breaks in bacteriophage T4. Journal of bacteriology. 1995; 177:6844–6853. [PubMed: 7592477]
29. Kuzminov A. Collapse and repair of replication forks in *Escherichia coli*. Mol Microbiol. 1995; 16:373–384. [PubMed: 7565099]
30. Halazonetis TD, Gorgoulis VG, Bartek J. An oncogene-induced DNA damage model for cancer development. Science. 2008; 319:1352–1355. [PubMed: 18323444]
31. Wach A, Brachat A, Pohlmann R, Philippsen P. New heterologous modules for classical or PCR-based gene disruptions in *Saccharomyces cerevisiae*. Yeast. 1994; 10:1793–1808. [PubMed: 7747518]
32. Guthrie, C.; Fink, G. Guide to Yeast Genetics and Molecular Biology. San Diego: Academic Press; 1991.
33. Oh SD, et al. Stabilization and electrophoretic analysis of meiotic recombination intermediates in *Saccharomyces cerevisiae*. Methods Mol Biol. 2009; 557:209–234. [PubMed: 19799185]
34. Friedman KL, Brewer BJ. Analysis of replication intermediates by two-dimensional agarose gel electrophoresis. Methods in enzymology. 1995; 262:613–627. [PubMed: 8594382]
35. Goldstein AL, McCusker JH. Three new dominant drug resistance cassettes for gene disruption in *Saccharomyces cerevisiae*. Yeast. 1999; 15:1541–1553. [PubMed: 10514571]

36. Conti C, Caburet S, Schurra C, Bensimon A. Molecular combing. Curr Protoc Cytom. 2001; Chapter 8(Unit 8 10)

37. Mann H, Whitney D. On a test of whether one of 2 random variables is stochastically larger than the other. Annals of Mathematical Statistics. 1947; 18:50–60.

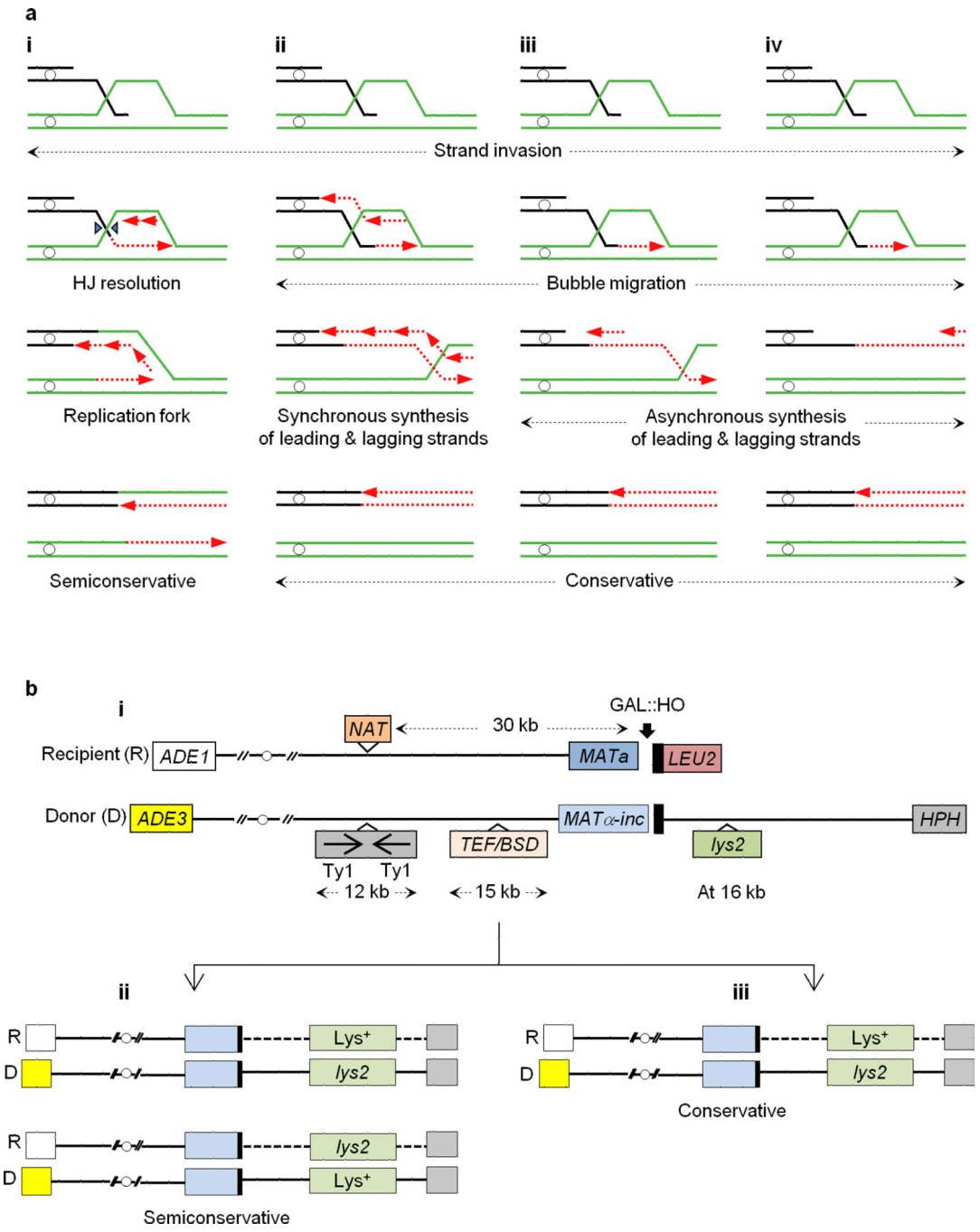

Figure 1. The mode of DNA synthesis during BIR

a, The models of BIR. **(i),** Replication fork proceeds semiconservatively. **(ii–iv),** Migrating bubble leads to conservative inheritance of new DNA. Synchronous **(ii)** and asynchronous **(iii,iv)** synthesis of leading and lagging DNA strands. **b, (i),** The BIR frameshift mutation assay. A DSB is induced at *MAT***a** of the recipient chromosome (Chr) III. *lys2* reporter is inserted in the donor chromosome 16 or 36 kb telomere-proximal from *MAT*α*-inc*. Lys^+ mutations would be inherited equally by the donor (D) or recipient (R) if BIR is semiconservative **(ii)**, but only by recipient if BIR is conservative **(iii)**.

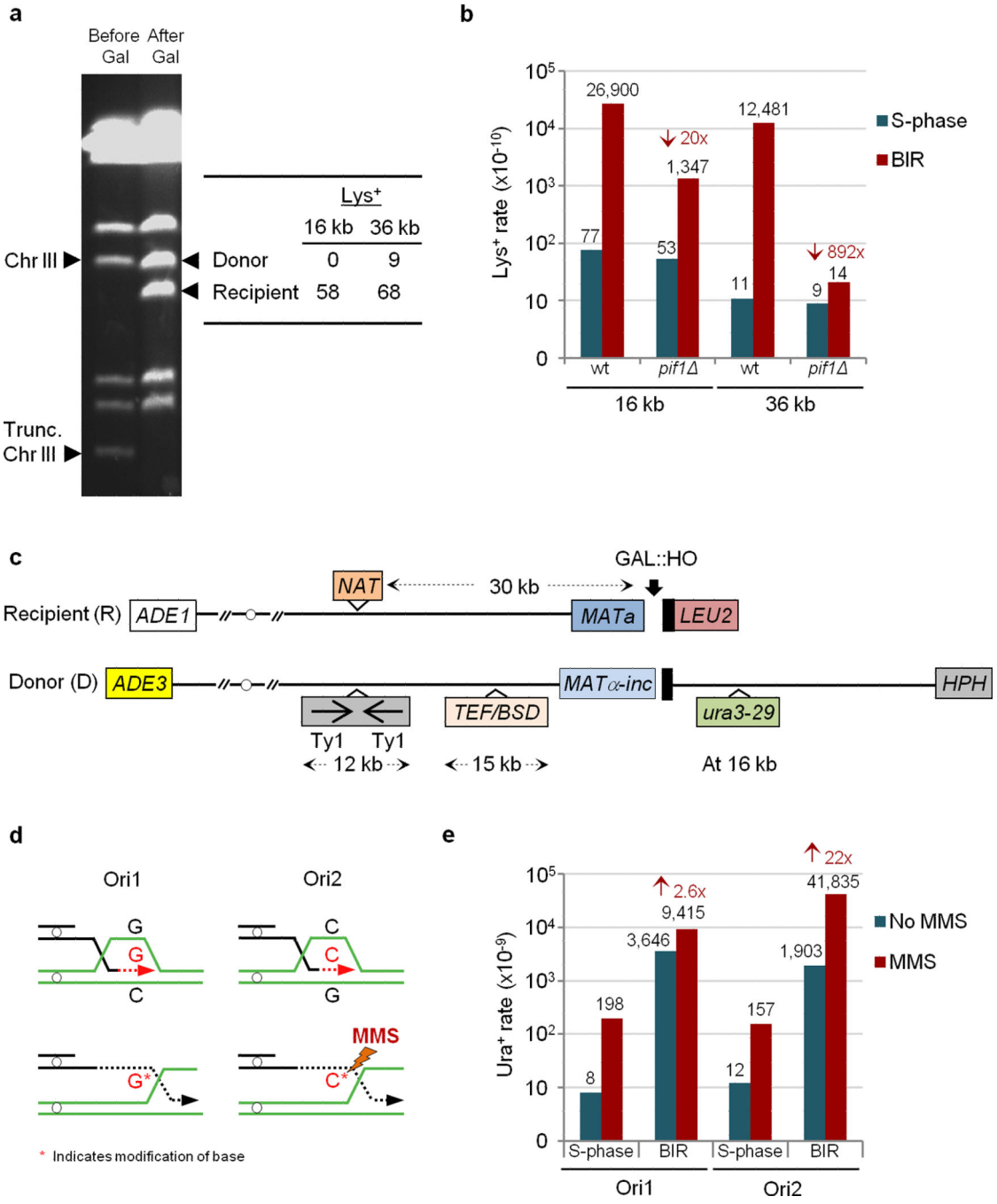

Figure 2. BIR-induced mutations

a, The sequencing of the separated donor and recipient chromosomes of heterozygous Lys$^+$ mutants. **b,** The effect of *pif1*Δ on BIR-induced frameshifts. Medians of mutation rates are shown. The arrows represent a reduction as compared to wt. **c,** The assay to study BIR-induced base substitutions in *ura3–29* reporter. **d,** Depending on orientation, the selectable position of *ura3–29* leading strand includes cytosine (C) or guanine (G). **e,** MMS amplifies BIR-induced base substitutions in orientation-dependent way. The arrows indicate an

increase as compared to no-MMS control. See Extended Data Tables 1 and 2 for the details of statistical analysis and for the ranges of medians shown in e and b.

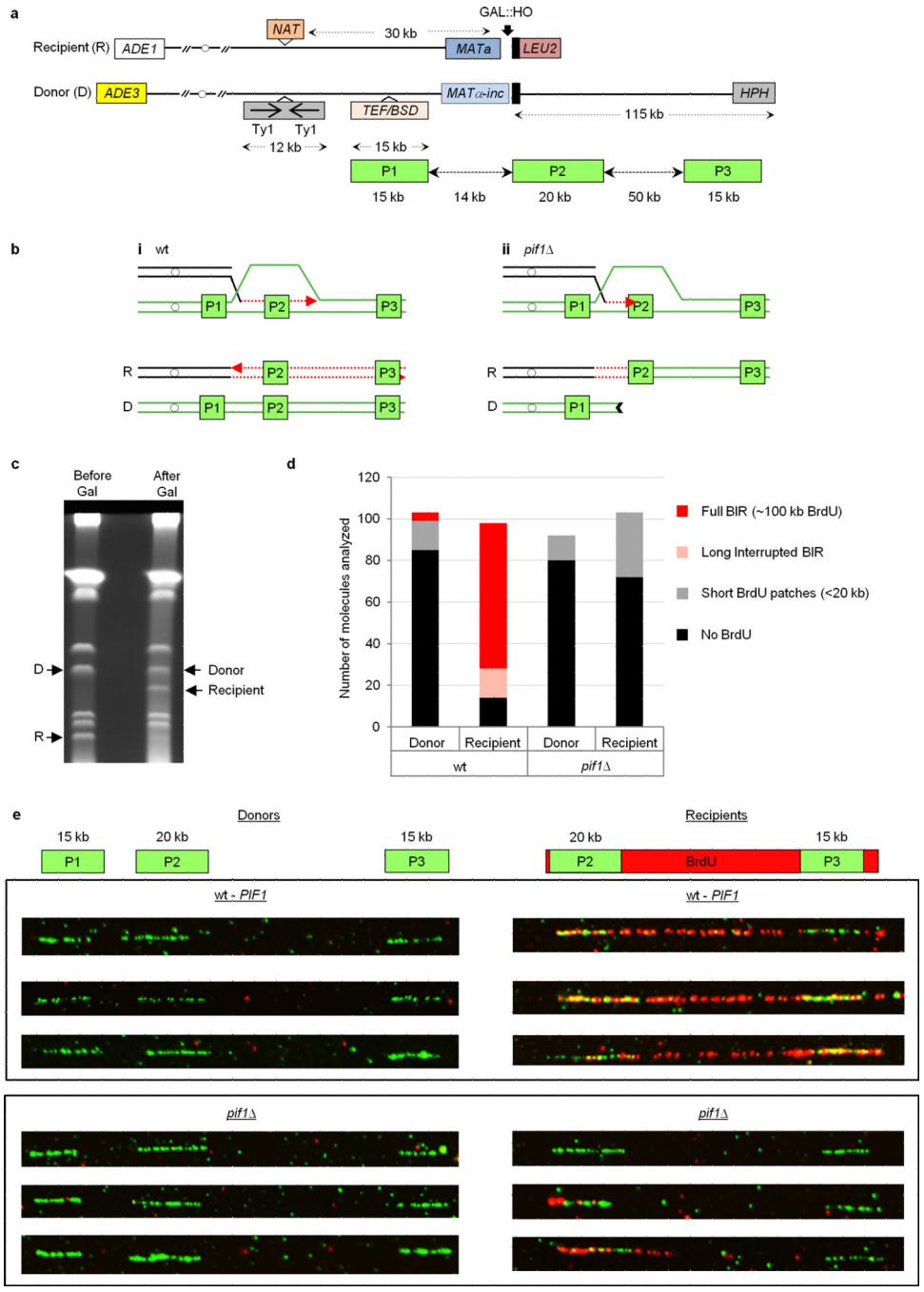

Figure 3. DNA synthesis during BIR is conservative

a, Experimental system to assay BIR using dynamic molecular combing including the position of hybridization probes P1, P2 and P3. **b, (i),** BrdU incorporation in the recipient is expected from conservative BIR (red). **(ii),** Formation of half-crossovers in *pif1*Δ leads to short patches of BrdU in recipient. **c,** Donor and recipient chromosomes separated using PFGE. **d,** The summary of molecular combing analysis. **e**, The donors and recipients of wt (*PIF1*) and *pif1*Δ. Each molecule was hybridized with P1, P2, P3 probes (green tracts) and treated with anti-BrdU antibodies (red tracts).

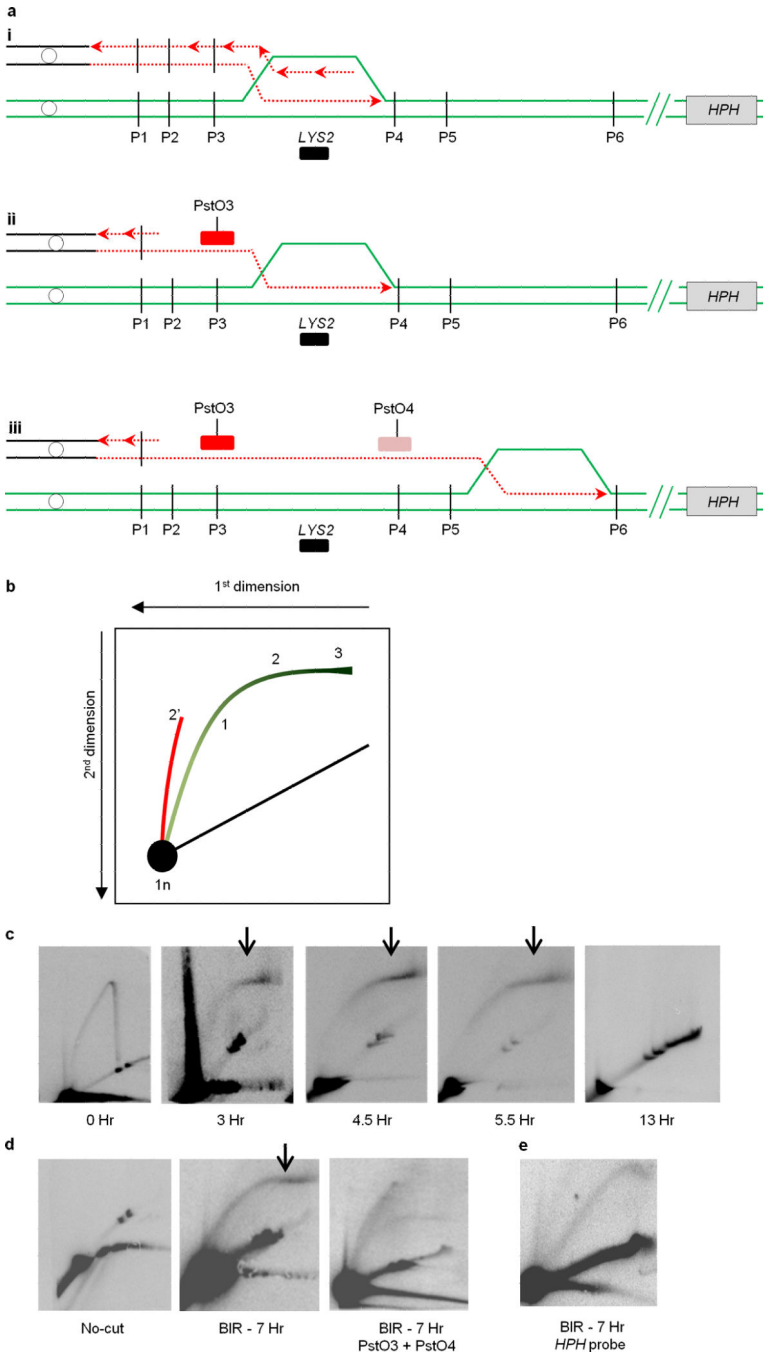

Figure 4. Molecular intermediates of BIR

a, D-loop migration during coordinated **(i)** and uncoordinated **(ii, iii)** leading- and lagging-strand synthesis. **b.** Schematic of 2D gel with BIR bubbles forming an arc (1,2) with an extension (3) representing ssDNA tail. Annealing with PstO3 and PstO4 allows PstI digestion changing the mobility of the intermediate (red, 2'). **c,** 2D analysis of Y-arc during normal replication (0Hr) and bubble-like structures at time points following BIR induction hybridized to *LYS2*-specific probe. **d,** High molecular-weight tails (arrows) disappear

following annealing with PstO3 and PstO4. The arc is absent in no-cut controls. **E**, BIR intermediates highlighted with *HPH*-specific probe.